Carbohydrate Polymer Technologies and Applications 7 (2024) 100440

Contents lists available at ScienceDirect

Carbohydrate Polymer Technologies and Applications

journal homepage: www.sciencedirect.com/journal/carbohydrate-polymer-technologies-and-applications

# Formulation and assessment of penetration potential of Risedronate chitosan nanoparticles loaded transdermal gel in the management of osteoporosis: *In vitro* and *ex vivo* screening

Sandhya Pathak [a], Prashant Sahu [b], J.P. Shabaaz Begum [c], Sushil K Kashaw [d,*], Archana Pandey [a,*], Prabhakar Semwal [e,f], Rohit Sharma [g,*]

[a] Department of Chemistry, Dr.HarisinghGour Central University, Sagar, (M.P.), 470003, India
[b] Babulal Tarabai Institute of Pharmaceutical Science, Sagar, (M.P.), 470228, India
[c] Department of Microbiology, Graphic Era Deemed to be University, Dehradun, (U.K.), 248002, India
[d] Department of Pharmaceutical Sciences, Dr.HarisinghGour Central University, Sagar, (M.P.), 470003, India
[e] Department of Biotechnology, Graphic Era Deemed to be University, Dehradun, (U.K.), 248002, India
[f] Research and Development Cell, Graphic Era Hill University, Society Area, Dehradun, (U.K.), 248002, India
[g] Department of Rasa Shastra and Bhaishajya Kalpana, Faculty of Ayurveda, Institute of Medical Sciences, Banaras Hindu University, Varanasi, 221005, Uttar Pradesh, India

ARTICLE INFO

*Keywords:*
Transdermal gel
chitosan nanoparticles
osteoporosis
release kinetics
Risedronate
ex vivo

ABSTRACT

Osteoporosis targeting by transdermal distribution has drawn a lot of attention as a cutting-edge, environmentally friendly platform for sustainable pain management. We investigate a novel biocompatible transdermal gel (RCNGL) containing biodegradable chitosan nanoparticles and Risedronate (RS) to treat osteoporosis. The RCNGL was formulated using the Pluronic F 127 co-polymer system and the ionic gelation process. The formulation showed a robust architecture of nanoparticle dispersion with a nano-size range of 201.8 nm when it was thoroughly analysed for Scanning Electron Microscopy, Dynamic electron Microscopy and transmission electron microscopy. At various temperatures, the entrapment efficiency was 67.53±1.05% with steady rheology and respectable porosity, validating FT-IR spectra that showed structural compatibility of RS with other excipients. The drug release test resulted in an 88% RS gel release, supporting sustained release kinetics. The *ex vivo* Franz diffusion study and *in vitro* cell uptake and distribution experiments revealed clear cell uptake and distribution with notable skin permeation displaying >70% RS release in mouse epidermal tissue. Overall, our research shows that biodegradable RCNGL may offer a potential osteoporosis and pain control strategy in clinical platforms using passive targeting.

## 1. Introduction

Osteoporosis is a progressive skeletal ailment diagnosed by low bone density and deterioration of bone tissues, with a consequent increase in bone fragility and susceptibility to fracture. Osteoporosis is called a "Silent disease" due to its symptoms unable to identify at early stage and leading to bone fractures. The fractures caused by osteoporosis have a great impact on public health (Tella & Gallagher, 2014; Zhang, Wei, Miron, Shi, & Bian, 2016). Currently most drugs available in the markets decrease bone loss by inhibiting bone desorption, but the novel therapies may increase bone mass by directly increasing bone mass as is the case of parathyroid hormone. Present treatment of osteoporosis includes bisphosphonates, calcitonin, selective estrogen receptor modulators and sufficient intake of calcium and vitamin D. Newer osteoclast targeted agents like Cathepsin K and C-SRC kinase are under clinical development (Fazil, Baboota, Sahni, Ameeduzzafar, & Ali, 2015; Schenk, Eggli, Fleisch, & Rosini, 1986). Bisphosphonates are the most commonly used drugs for the treatment of osteoporosis; the efficacy of this drug class for reducing the risks of osteoporosis has been well established in large clinical trials. Bisphosphonates are used to treat osteoporosis in the US and many other countries including India. Osteoclasts are the target cells of bisphosphonates, though the most drug-sensitive steps of their formation and activity have not been determined. Bisphosphonates (BPs) are highly hydrophilic compounds with low oral bioavailability having

* Corresponding authors.
*E-mail addresses:* Sushilkashaw@gmail.com (S.K. Kashaw), prof.archnapandey@gmail.com (A. Pandey), rohitsharma@bhu.ac.in (R. Sharma).

https://doi.org/10.1016/j.carpta.2024.100440

Available online 24 January 2024

the property of most effective bone resorption inhibitors. The mechanism of action of BPs is induction of apoptosis in osteoclasts (Sigua-Rodriguez, da Costa Ribeiro, de Brito, Alvarez-Pinzon, & de Albergaria-Barbosa, 2014; Watts, Ellims, & Eccleston, 2014). Risedronate monosodium salt (Sodium 1-hydroxy-1-phosphono-2- (pyridin-3-yl ethyl phosphonate) is a member of Class BCS (III), the third-generation BPs. Risedronate is an efficient anti- osteoporosis drug among other BPs, which reduces the gastro-intestinal (GI) side effects. It is more potent drug having good solubility in water, but poor oral bioavailability (less than 1%, about 0.63%) (Garzoni et al., 2004; Papapetrou, 2009). There are a number of drugs whose clinical development failed due to poor solubility, inadequate bioavailability, and other poor biopharmaceutical properties, so at present research work is going on to solve this problem. The major task in the development of these drugs is the improvement in solubility, thereby enhancing oral bioavailability. The most frequently applied nanotechnology-based strategies in the development of delivery systems are polymeric nanoparticles (NPs), solid lipid NPs, liposomes, nanoemulsions, nanosuspension, and micelles etc., which provide controlled, sustained, and targeted drug delivery. The NPs based delivery systems present a significant approach for enhancing solubility and oral bioavailability of drugs (Araujo, 2009; Dissette et al., 2010; Rao, Dandala, Lenin, Sivakumaran, Shivashankar, & Naidub, 2007). Chitosan is an important polymeric carrier for many drugs because of its specific properties such as polycationic nature, biodegradability, biocompatibility and non-toxic nature. Chitosan is a natural polysaccharide derived by the process of, "Deacetylation of chitin". Ion gelation is the commonly used method for the formulation of CS NPs. The electrostatic interaction between the amine group of chitosan and a negatively charged group of polyanion such as sodium tripolyphosphate (TPP) is the basic mechanism of this method. In many previous studies, it is reported that different drugs loaded CS nanoparticulate formulations are stable, permeable and therapeutically active (Guyot & Fawaz, 2000; Higuchi, 1963; Peppas, 1985).

In the current study we investigate the Risedronate- Chitosan nanoparticles loaded skin permeating biocompatible transdermal gel (RCNGL) for better bioavailability and acceptability of this drug to the biological systems. The RCNGL system is designed for promoting the therapeutic effect of a risendronate at very low clinical dose and evading the systemic and local toxic side effects by passive delivery. Additionally, local delivery enhance the direct absorption of risendronate at very low dose avoiding frequent dosing and contributing patience compliance. The RCNGL was synthesized by ion gelation–Pluronic F 127 gelling system and were characterized for average particle size, surface charge, size distribution, drug entrapment efficiency and in-vitro drug release. Since the formulation strategy involves no electromobility during the synthesis process the complete formulation showed eco-friendly synthesis with no production of toxicity and local adverse effects. The effect of formulation variables such as CS, TPP & Pluronic 127 and process parameters like stirring speed, sonication time and interval on the drug entrapment efficiency and particle size was measured (Hirabayashi, Sawamoto, Fujisaki, Tokunaga, Kimura, & Hata, 2002; Peppas, 1985; Qiu, Chen, Zhang, Yu, & Mantri, 2016; Sahu, Das, Mishra, Kashaw, & Kashaw, 2017).

## 2. Materials and Methods

### 2.1. Materials

The drug Risedronate-sodium (M.W. of 305.09 g/ mol.) was procured from Sigma Aldrich. (Mumbai, India). Chitosan with medium molecular weight (M.W. =750 000 Da) was purchased from Himedia (India). Pluronic F 127 was purchased from Sigma Aldrich, Bengaluru, India. Dialysis membrane (Mol. wt. cut-off: 12 000 Dalton, flat with 25 mm, diameter of 16 mm) was purchased from Himedia (India). High purity water was used for all experiments, prepared by using (Millipore). All other chemicals and reagents were of analytical grade.

### 2.2. Preparation of skin permeating Risedronate loaded Chitosan Nanoparticles (NPs) Transdermal gel (RCNGL)

Risedronate loaded Chitosan nanoparticles were prepared by the ionic gelation method (Stamatialis et al., 2008). Accurately CS (0.4% w/v) was dissolved in aqueous acetic acid (2% v/v) solution and stirred well up to complete dissolution then filters it with 0.2 μ filter paper. The pH was adjusted up to 4.8-5.0 by adding 0.1 M NaOH solution. A fix amount of drug (20 mg) was added in polymeric solution post adjusting the pH. The drug loaded chitosan NPs were prepared by the drop wise addition of TPP solution to the polymeric solution at room temperature on magnetic stirring for 3-4 hours. The optimization parameters such as CS concentration, TPP concentration, stirring speed and pH for nanoformulation were optimized. The prepared NPs suspension was analyzed by transmission electron microscopy (TEM) and Dynamic light scattering (DLS) for particle size. The optimized NPs suspension was centrifuged at 15000 rpm for 30 min using cooling centrifuge ($C_{24}$, Remi Centrifuge, and Mumbai (India). The pellets were freeze-dried and stored at 5 ± 3°C. The weights of freeze-dried nanoparticles were also measured. The nanoformulation was further optimized for the formation of stable and optimum dosed transdermal gel (Choi, Gang, Chun, & Gwak, 2008). The Pluronic F-127 gel was prepared by dissolving 20 % w/v Pluronic F-127 in cold water with constant stirring for 2 h followed by overnight preservation in refrigerator (2–8 °C) resulted in clear solution from hazy appearance (Sahu, Sushil, Samaresh, & Arun, 2017). Dried 100 mg Risendronate encapsulated chitosan nanoparticles were added in Pluronic F-127 gel system followed by stirring for 2 h for the final synthesis of skin permeating transdermal gel (RCNGL) (Kusamori et al., 2010).

## 3. Characterizations of synthesized Risedronate Chitosan Nanoparticles transdermal gel (RCNGL)

### 3.1. Transmission Electron Microscopy (TEM)

The TEM of the synthesized RCNGL was performed by using Hitachi H-7500 TEM instrument. The TEM images were performed to visualize the shape and size of prepared formulation, coated with 2.5% w/v of Phosphotungstic acid (PTA) solution and placed in a copper disc grid. The grid was then dried in 60 watt LED lamp (Philips, India Ltd) and was finally placed in the disc holder and scanned for the transmission electron microscopy analysis (Nam et al., 2011).

### 3.2. Scanning Electron Microscopy (SEM)

The arrangement, morphology and orientation of synthesized RCNGL was assessed by using scanning electron microscopy (SEM), Nova Nano SEM 450, Germany. Prior to the SEM evaluation, the synthesized formulation was lyophilised by using freeze dry lyophilizer, REMI, New Delhi, India. The RCNGL nanoformulation was placed on SEM stub by employing the double sided adhesive tape at 50 mm for 5-10 min via sputter (KYKY SBC-12, Beijing, China) (Sahu, Kashaw, Kushwah, Sau, Jain, & Iyer, 2017). A SEM aided with secondary electron detector was employed to obtain the digital images of the developed drug loaded gel system.

### 3.3. Particle Size, Dynamic Light Scattering (DLS) and Poly-dispersity Index (PDI) Analysis

The particle size, surface charge and PDI of the synthesized RCNGL were assessed by Malvern Zetasizer 3000 (Malvern Instruments, Bedfordshire, UK). The Zeta potential was measured by applying the electrophoretic mobility principle of particles in an applied electrical field. The concentration of the RCNGL was adjusted to 0.01% w/v by using distilled water in 0.01 M sodium chloride solution for potential assessment (Pasqualone, Oberti, Andreetta, & Cortizo, 2013). The DLS

analysis was carried out for the more distinct and persuasive evaluation of the RCNGL was assessed at wavelength 330 nm at a temperature of 25 °C (Fleisch, 2000). The formulation, analysis was triplicated and average of triplicated data along with SD was reported.

### 3.4. Fourier Transform Infra-Red (FTIR) analysis

The FTIR device of Perkin Elmer (Waltham, Massachusetts, USA) was employed for FTIR spectral analysis of Risedronate drug (API), polymer (chitosan), TPP, and Risedronate loaded chitosan nanoparticles (RS-CS NPs) for the qualitative determination of chemical structure of individual candidates and elucidate the chemical interaction between polymer and API. The components were lyophilized to get dry powder and the obtained dried powder was mixed with KBr and pressed to plate for assessment (Das, Sahu, Chaurasia, Mishra, & Kashaw, 2018).

### 3.5. DSC (Differential Scanning Colorimetry), TG (Thermogravimetry) and DTA (Differential Thermal Analysis)

The DSC was employed for the compatibility evaluation of individual components (drug and polymer) and for the determination of physiochemical stability analysis. The thermogram were obtained for API Risendronate, drug loaded nanoparticles by using a Shimadzu DSC-50 system (Shimadzu, Kyoto, Japan). About 2.0 mg of samples were crimped in a standard aluminium pan and heated from 20 to 350 °C at a heating constant rate of 10 °C/min under constant purging of nitrogen at 20 mL/min (Li et al., 2014). The formulation, analysis was triplicated and the measurement was repeated as an average of triplicated value with SD.

### 3.6. Rheology and Stability of Gel

Viscoelastic behaviour of the synthesized RCNGL was studied using programmable Rheometer (Brookfield DV III ultra). Data analysis was carried out by employing Rheocalc V.2.010. The synthesized RCNGL sample was equilibrated prior to each reading. Continuous shear investigation was done with rheometer having CP41 spindle with cone and plate geometry as a measuring system (Cione, Liberale, & Silva, 2010). Shear rate was increased from 0–60 D in ascending order as well as in descending order to obtain up and down curves. The resultant shear stress was measured accordingly (Olkin & Pratt, 1958). The formulation was subjected to stability studies. The RCNGL sample was stored at 8 °C, 25 °C, 32 °C and 45 °C for three months to access their stability.

### 3.7. Drug Entrapment Efficiency

The drug entrapment efficiency of the developed RCNGL was calculated by the absorption and extraction method. The RCNGL was weighed 100 mg with accuracy and mixed in 50 mL of acetonitrile. This mixture was then kept at magnetic stirrer for 1h at room temperature. The obtained suspension was filtered using 0.45 μm membrane filter. The filtrate was checked by the UV spectrophotometric analysis at $\lambda_{max}$ 262 nm and following formula was applied for the quantitative estimation of entrapment efficiency (Prashant Sahu, 2017):

$$\%\ Drug\ Encapsulation\ Efficiency = \frac{Drug\ in\ formulation\ after\ extraction}{Theoretical\ drug\ in\ formulation} x100$$

### 3.8. Sol-Gel Fraction & Porosity Analysis

The RCNGL was checked for the sol and gel fraction using Soxhlet extraction setup where they kept for 4 h with water at 80 °C. Recollected gel was dried in vacuum oven at 45 °C till constant mass. Following formulas were applied to calculate the sol and gel fractions (Damle & Birajdar, 2015).

$$\%\ Sol\ Fraction = \frac{Wo - Wt}{Wo} x\ 100 \ldots\ldots\ldots \quad (a)$$

$$\%\ \text{Gel Fraction} = 100 - \text{Sol Fraction} \ldots\ldots \quad (b)$$

Whereas in sol fraction, $W_0$ is weight of gel before extraction and $W_t$ is the weight after extraction.

Porosity of the RCNGL was measured by fluid displacement method. Initially, pre-weighed oven dried RCNGL was immersed in distilled water till saturation and change in the weight was marked. Saturated RCNGL was blotted and the weight variation was calculated. Following mathematical tool was employed to calculate % porosity (Ritger & Peppas, 1987).

$$\%Porosity = \frac{Ws - Wd}{\rho V} x100$$

Where, Ws is the weight of saturated gel, Wd is the weight of dried gel, ρ is distilled water density and V is volume of respective formulation.

### 3.9. In-vitro drug release studies

The in-vitro drug release studies of the RCNGL was performed by using the dialysis bag with shaking incubator (REMI, New Delhi, India). Saline phosphate buffer with pH 5 was used as a dissolution medium to mimic the skin microenvironment, for effective topical delivery (Costa & Lobo, 2001). The normal skin surface pH is unerringly 5 was and skin epidermal cell pH is 7.4. The two pH analysis was performed to analyze the negligible effect of nanoformulation towards the normal skin cell. Each dialysis bag (pore size: 12kD; Sigma Chemical Co., St Louis, MO) were loaded with about 5 mL of RCNGL sample previously filtered through the Sephadex Column G-50. The volume and temperature of dissolution medium were 50 mL, and 37±2 °C, respectively. At the predetermined time interval 5 mL of sample was withdrawn, replaced with the same volume of fresh media, filtered and measured for the drug content at 262 nm against blank using UV–Visible spectrophotometer (Borah, Deka, & Duary, 2017). The following equation was employed to calculate the risendronate release from the nanoparticles:

$$\textbf{\textit{Amount of Risendronate release}}\ \left(\frac{\textbf{\textit{mg}}}{\textbf{\textit{ml}}}\right) = \textbf{\textit{Concentration X Dissolution bath volumeX dilution factor}} \Big/ 10000$$

Also

$$\textbf{\textit{Cumulative Percentage release}}(\%) = \textbf{\textit{Volume of sample}} \frac{\textbf{\textit{withdrawn}}}{\textbf{\textit{bath volume x p}}(t-1) + \textbf{\textit{Pt}}}$$

Where, Pt = Percentage release at time t
Where P (t – 1) = Percentage release previous to‘t’

### 3.10. Stability Analysis

The stability studies of the developed RCNGL was carried out by

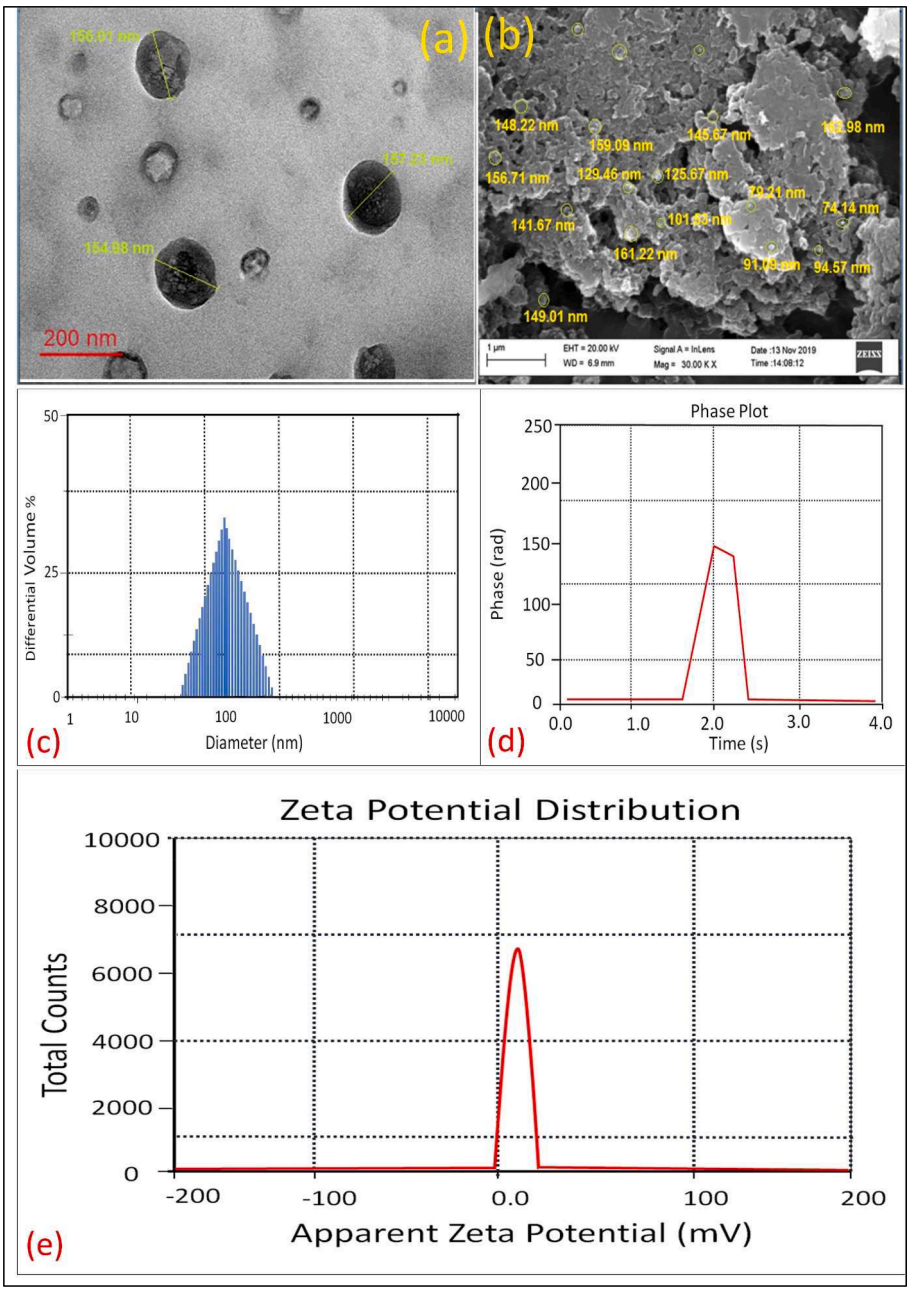


**Fig. 1.** Image I elaborating TEM analysis of Risendronate chitosan nanoparticles at 100 nm scale bar, image I b demonstrating SEM evaluation of RCNGL, whereas images I (c-e) demonstrating DLS, average particle size and zeta potential of developed Risendronate chitosan NPs, (Mean ± SD, n=3).

storing the gel formulation in amber coloured glass bottles at 4±1 °C, 25 ±2 °C and 40±2 °C for a period of 45 days and observed for the change in particle size and surface morphology. Over the storage period of 45 days the physical, chemical, microbiological, and morphological changes were measured, ultimately deciding the stability and therapeutic potential of gel (Wong et al., 2019).

### 3.11. *In-Vitro Cell Culture Assay*

#### 3.11.1. *Cell Culture and Cell Seeding*

Normal Human dermal fibroblast (NHDF) cell line was obtained from NCCs Pune and was preserved in Dulbecco's modified Eagles Medium (DMEM). The cell line was then augmented with 10% fetal bovine serum (FBS) and 100 U/mL penicillin, and 100 µg/mL streptomycin (PAA Laboratories GmbH, Austria) antibiotic solution. The NHDF cell line was harvested in tissue culture flasks (75 $cm^2$) and preserved at 5% $CO_2$ atmosphere at 37 °C. After reaching the 90% confluency, the cells were trypsinized with 0.25% trypsin EDTA solution (Sigma, USA) (Sahu et al., 2019).

#### 3.11.2. *Cell uptake Assay by CLSM*

The advanced uptake and distribution studies were executed by using confocal laser microscopy (CLSM) for understanding the distribution capability of RCNGL using NHDF cell lines. The cells were incubated with RCNGL (equivalent to 1 µg/ml) for 3 h. After incubation, the media comprising the RCNGL was washed with Hanks buffered salt (HBS) solution (PAA Laboratories GmbH, Austria) three times and were detected under CLSM (Olympus FV1000) (Tanwar, Chauhan, & Sharma, 2007).

#### 3.11.3. *MTT Assay*

MTT assay was employed to analyze the cell cytotoxicity of the

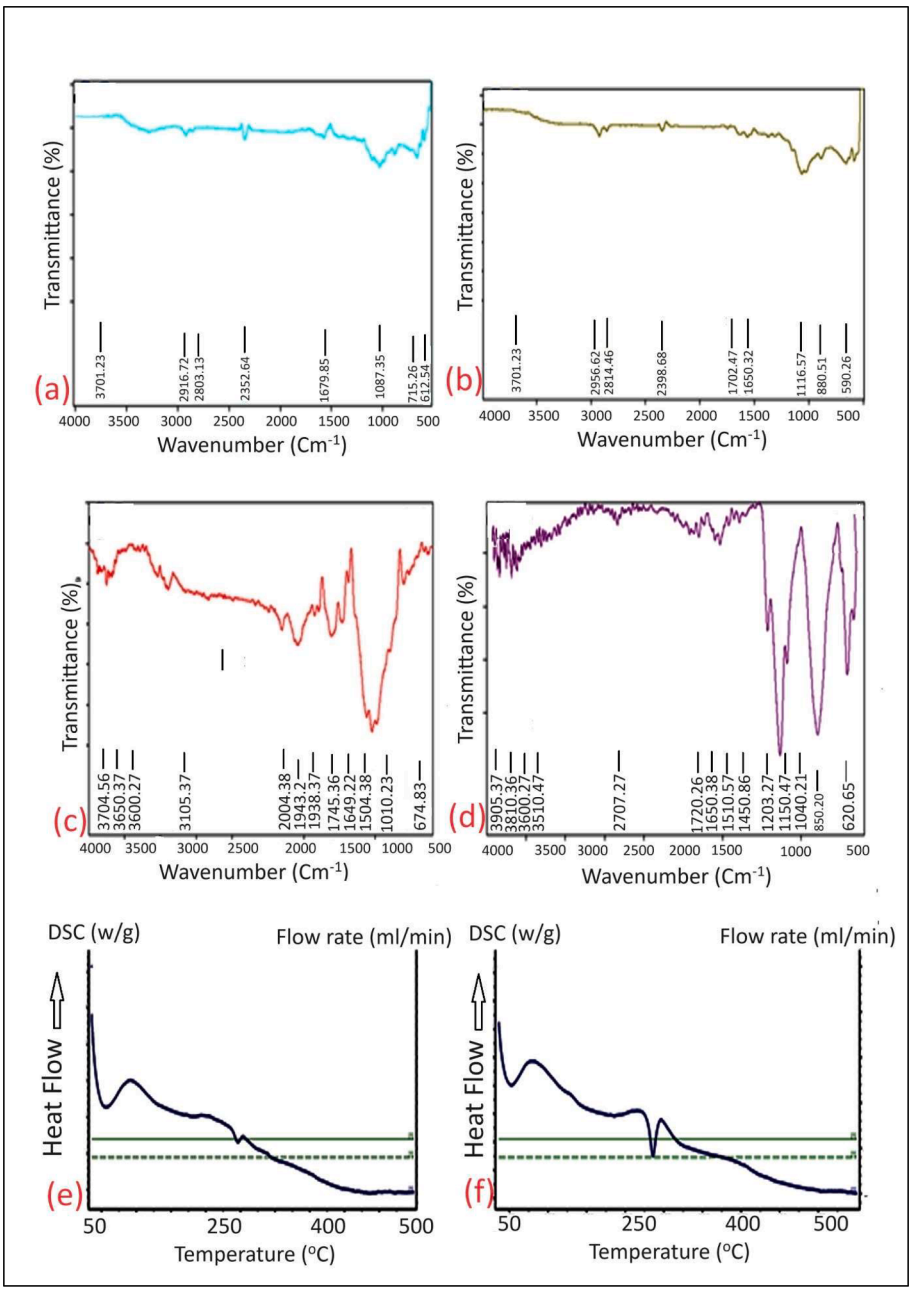


**Fig. 2.** Images a-d elaborating FTIR analysis of free drug Risedronate, chitosan, TPP, and Risedronate loaded chitosan nanoparticles with different absorbance range, Images e-f showing quantitate DSC analysis of free drug Risendronate and developed chitosan NPs, (Mean ± SD, n=3).

developed RCNGL in NHDF cell line. Briefly, NHDF cell line was seeded in 96 well plates and incubated with media containing free drug Risendronate, blank NPs and RCNGL (equivalent concentration of 0.1,1.0, 2.0 and 5.0 μg/mL), negative control (cells treated with blank media) and positive control (Triton X-100). After 24 h of incubation, the media encompassing the samples were enunciated and cells were washed with HBSS three times. Subsequently, 150 μL of the MTT solution (500 μg/mL in PBS) was added to each well and re-incubated for 4h. After 4 h the MTT solution was carefully articulated and the formazan crystals were then dissolved in 200 μL of DMSO. The optical density (OD) of the resultant solution was then screened at 262 nm using an ELISA plate reader (Bio Tek, USA) (Liu, Chang, & Hung, 2011).

### 3.12. *Ex vivo* Skin Permeation Studies

#### 3.12.1. Skin Penetration Analysis

The skin permeation assay was carried out using male mouse epidermal tissue which was sliced into the optimal size by using a surgical scalpel (DISPO VAN, Hindustan syringes & medical devices, Faridabad, India) prior to the deep cleaning and removal of hair. The skin penetration potential of the free drug Risendronate and RCNGL were evaluated by observing the samples under a UV lamp prior tagging with Rhodamine 123 dye and compared for significant penetration. For the skin permeation assay, the tissue was sandwiched between the donor and acceptor compartment of the FD cell. About 1 mL Rhodamine 123 tagged free drug Risendrnate and RCNGL was added in the donor compartment. The PBS solution (pH 5) at temperature 37 °C was incessantly stirred serving as the acceptor compartment dissolution media. The test samples were withdrawn after 24 h and equivalent

amount of the PBS solution was replaced to maintain the optimum sink condition (Ballarin, Galli, Mogavero, & Morigi, 2011). The collected test samples were then analyzed for drug released by UV spectroscopy method.

#### 3.12.2. Drug Concentration-Depth Profile

The amount of drug relents on post release from the free drug Risendronate and RCNGL within the mouse tissue was evaluated by collecting the skin from the FD cell after the 24 h experimental exposure. The samples treated tissue was carefully washed with PBS solution (pH 5) and cut into 50μm size using cryotome. The tissue was then divided and designated into 3 layers as upper, middle and lower epidermal layers. The retained drug from the tissue was extracted by adding 5 mL ethyl alcohol, stirred for about 10 h and centrifuged for 20 minutes. The supernatant was collected and filtered via 0.2 mm syringe filter and analyzed for the drug content by UV spectrophotometry method (Ngo, Lee, Kim, & Kim, 2009).

#### 3.12.3. Histological Analysis

For the histological analysis, the experimental tissue sample was collected, washed thoroughly with a PBS solution (pH 5) and fixed by using 10% w/v formaldehyde solution. After the treatment with formaldehyde, the tissues were processed to eradicate the formaldehyde and sectioned by using microtome. Finally, the sectioned tissues were preserved and stained with hematoxylin and eosin dye and visualize under the microscope (Olympus, japan) (Dey, Banerjee, Sen, & Shankar, 2011).

### 3.13. Statistical analyses

The values were expressed as mean ± SD. Statistics. Statistical analysis of the data was performed via one-way analysis of variance (ANOVA) using origin software; a value of $p<0.01$ was considered significant, (n = 3) (Sahu, Kashaw, Jain, Sau, & Iyer, 2017).

## 4. Results and Discussion

### 4.1. Synthesis and mechanism of RCNGL

The RCNGL was synthesized by an ion-gelation method using sodium tripolyphosphate (TPP) as cross-linker with Pluronic 127 as solvent system. The ionic bonding between the core cationic amino group on chitosan backbone with amiable anionic phosphate group of TPP results in the robust chemical crosslinking portent (Ulbrich, Hola, Subr, Bakandritsos, Tucek, & Zboril, 2016). The copolymer of propylene oxide and ethylene oxide (Pluronic 127) is a hydrophilic copolymer. It produces monomolecular micelles at low concentration between 5-10 % w/v and multi-molecular clusters at higher concentration above 15 % w/v. The Pluronic 127 at gel phase exhibits a hydrophobic central core, exposing hydrophilic polyoxyethylene chain amiable to the external environment. Micelle formation of Pluronic-127 occurs above critical micellar concentration in the appropriate solvents system at optimal temperature. Above critical micellar concentration the micelles achieve a lattice configuration and form gel.

**Table 1**
**Demonstration of rheological parameters (Viscosity, Thixotropy & Flow index) of developed RCNGL at different temperature range and storage interval, (*, p > 0.01 ∅∅ and ## = non-significant, Mean ± SD, n=3).**

| S. No. | Studies | Time | Temperature | | | |
|---|---|---|---|---|---|---|
| | | | 8 °C* | 25 °C$^{\varnothing\varnothing}$ | 32 °C$^{\#\#}$ | 45 °C* |
| 1. | **Viscosity (cps)** | 0 month | 3899* | 3503$^{\varnothing\varnothing}$ | 3130$^{\#\#}$ | 2768* |
| | | 1 month | 3847* | 3439$^{\varnothing\varnothing}$ | 3011$^{\#\#}$ | 2604* |
| | | 2 month | 3780* | 3387$^{\varnothing\varnothing}$ | 2978$^{\#\#}$ | 2570* |
| | | 3 month | 3610* | 3279$^{\varnothing\varnothing}$ | 2835$^{\#\#}$ | 2447* |
| 2. | **Thixotropy (Dynes/cm$^2$.S$_)$** | 0 month | 7389* | 7290$^{\varnothing\varnothing}$ | 7137$^{\#\#}$ | 6924* |
| | | 1 month | 7303* | 7200$^{\varnothing\varnothing}$ | 7098$^{\#\#}$ | 6891* |
| | | 2 month | 7269* | 7087$^{\varnothing\varnothing}$ | 6988$^{\#\#}$ | 6845* |
| | | 3 month | 7188* | 7002$^{\varnothing\varnothing}$ | 6911$^{\#\#}$ | 6800* |
| 3. | **Flow index** | 0 month | 0.66* | 0.65$^{\varnothing\varnothing}$ | 0.65$^{\#\#}$ | 0.64* |
| | | 1 month | 0.64* | 0.63$^{\varnothing\varnothing}$ | 0.63$^{\#\#}$ | 0.62* |
| | | 2 month | 0.62* | 0.60$^{\varnothing\varnothing}$ | 0.59$^{\#\#}$ | 0.59* |
| | | 3 month | 0.60* | 0.58$^{\varnothing\varnothing}$ | 0.57$^{\#\#}$ | 0.55* |

### 4.2. TEM

The TEM analysis showed round and even nanoparticles arrangement, legalising the oval shape of prepared RCNGL (Fig. 1 a). The TEM results analysis validate the shape and size distribution pattern of RCNGL with a slight accumulation of particles due to the hydrophilic nature of chitosan polymer. The average particle size of RCNGL was found to be 156 ±0.11 nm, when analyzed by J software conforming the zeta-sizer outcomes. The TEM analysis showed significant nanosize distribution of RCNGL particles for the enhanced operative topical delivery and significant intracellular transport.

### 4.3. SEM

The SEM outcomes established broader analysis of the RCNGL regarding shape and the surface consistency. The outcomes of the SEM analysis confirming the oval architecture of RCNGL, thereby authorising the TEM investigation. The SEM images showing strong round shape of the RCNGL with a slight constellation of particles again establishing the hydrophilic nature of RCNGL chitosan polymer structure. The size range exemplified by the SEM investigation of RCNGL was found between 145-158 nm with average size of 152 ± 1.68 nm when calculated by J software (Fig. 1 b) authorising the TEM results.

### 4.4. Particle Size, Dynamic Light Scattering (DLS) & Poly-dispersity Index (PDI)

The zeta sizer analysis showed distinct size range of RCNGL between 100-120 nm. The smaller size of the RCNGL displayed optimum entrapment of Risendronate within the polymer (Chitosan) matrix due to the formulation and process optimization. The surface charge of RCNGL was + 22.31 mV demonstrated cationic nature of RCNGL. The zeta potential befalls between 40-60 mV exhibiting noteworthy stability for efficient transdermal delivery. The pH of RCNGL was found to be 5.2 ± 0.42 which play a vital role in acid activation and served as a driving force for the competent topical delivery via skin surface. The pH triggered mechanism act as the key element for the onsite degradation of the polymer matrix. This pH based topical delivery results in the enhanced drug release at a sustained rate leading to desired therapeutic potential and elimination of local cellular toxicity. The DLS results showed sharp and detailed size distribution pattern of RCNGL. The nanosize of RCNGL showed an enhanced delivery to the dermal area and personified the size of cells and its micro-environment. The DLS investigations displayed varied size distribution of RCNGL between 135-160 nm and exhibited PDI of 0.152 ± 0.09 (Fig. 1 c-e). The nano size range facilitates better diffusion of RCNGL across the skin barricades leading to desired therapeutic potential at targeted site. The DLS outcomes significantly validated the results of zeta sizer endorsing RCNGL for stable and ideal nanocarrier for effective transdermal delivery.

### 4.5. Fourier Transform Infra-Red (FTIR)

The FTIR spectra of the Risedronate drug (API), polymer (chitosan), TPP, and Risedronate loaded chitosan nanoparticles (RS-CS NPs) are shown in fig. 2 a-d. The drug Risedronate sodium showed the specific peak at 1028.56 $cm^{-1}$., which indicates aliphatic P = O stretching. The peaks at 2923.91 $cm^{-1}$ and 1028.56 $cm^{-1}$ is because of C–H stretch and aromatic P= O stretch, respectively. C=C and C=N stretch was

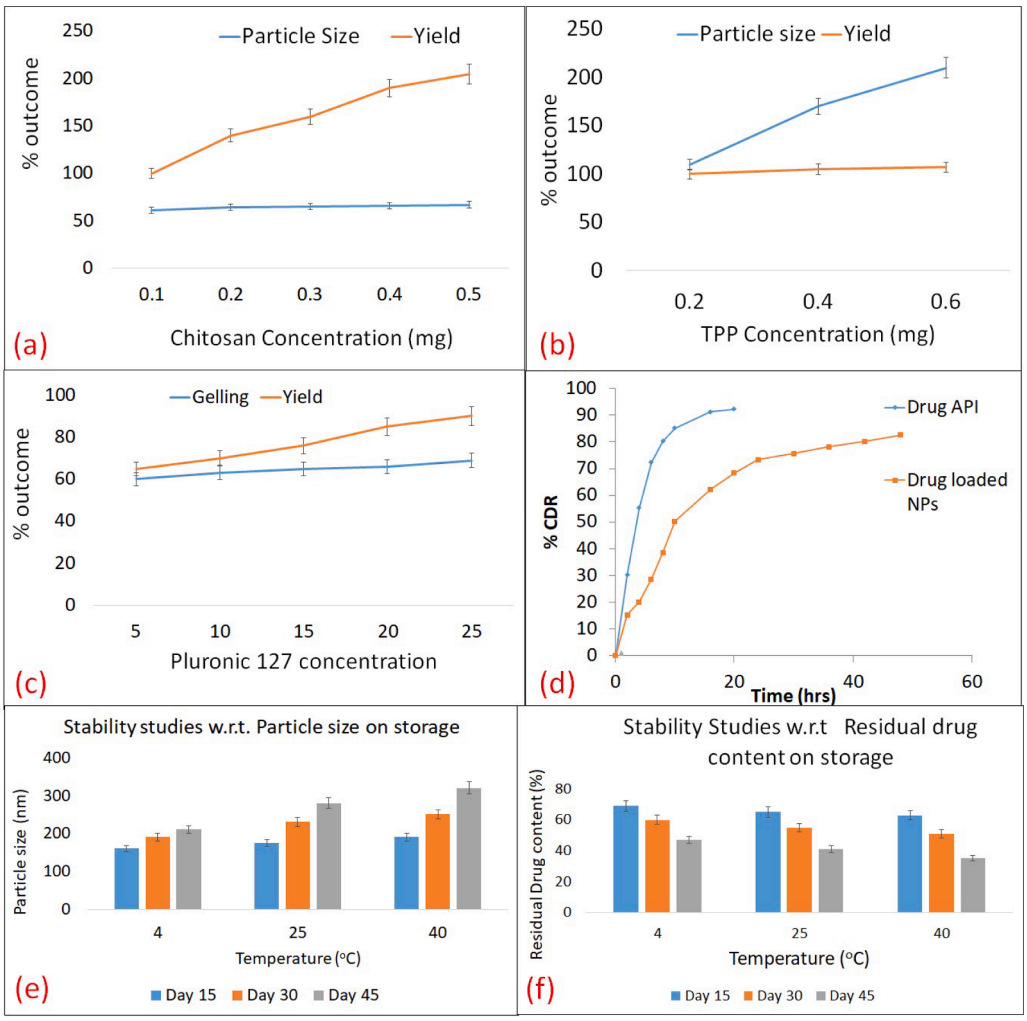


**Fig. 3.** Images (a-c) showing sol–gel fraction analysis of Risendronate, Chitosan and TPP concentration exhibiting yield and gelling stage, whereas image (d) showing in vitro drug release of pattern of free drug Risendronate and RCNGL at pH 5, images e-f displaying stability studies of RCNGL w.r.t to particle size and residual drug content at varied temperature range on storage, (mean ± SD, n=3).

characterized by the peaks between 1400 and 1600 cm-1. Chitosan showed a well-defined peak at 2890 $cm^{-1}$ due to C-H stretching, 1546 $cm^{-1}$ for N-H bending, and 1304.22 for C-N stretching. TPP showed the featured peaks at 1213.77 $cm^{-1}$ for P=O Stretching, 1133.87 $cm^{-1}$ due to O−P=O Vibrations, and 896.79 $cm^{-1}$ for Stretching vibration of the P−O−P bridge. The FTIR spectra of RS-CS NPs showed separately identified peaks. It reveals that there was no chemical interaction between the drug and polymers.

### 4.6. Differential scanning calorimetric (DSC) study

Differential scanning calorimetry (DSC) thermogram of risedronate sodium is shown in the fig. 2 (e & f). Differential scanning calorimetric (DSC) studies indicate a sharp endothermic peak at 250°C (approx.) corresponding to the melting point of the sample (262°C) which matches with the melting point of risedronate sodium indicating the identification of the drug. From the DSC thermogram of pure drug and drug loaded NPs it is clearly shown that, the drug did not form a complex with the excipients as the endothermic peaks remained unchanged in position.

### 4.7. Rheology and stability Analysis

The rheological pattern of the synthesized RCNGL was measured at varying temperature i.e., 8 °C, 25 °C, 32 °C and 45 °C on incubation at 1, 2 and 3 months. The viscosity, thixotropy and flow index was assessed and demonstrated in the table 1. The rheological pattern obtained at 25 °C and 32 °C is regard as the standard temperature for the effective transdermal delivery as 25 °C regard as room temperature and 32 °C is falls close to skin temperature. The outcomes established the declining trend in all three rheological profile equated with time interval and temperature. The decline in rheology was slight and non-significant confirming the greater physiochemical stability of RCNGL. The synthesized RCNGL showed significant resisted alteration in the viscosity as a function of storage interval and temperature resulting in decent thermal stability in gelling condition. Also, the variation in rheology was due to the drug loading, swelling and de-swelling of Pluronic F-127 gelling system. The decent crosslinking between the polymer network of exterior chitosan and co-polymer system of 3D gel network of Pluronic F-127 established better swelling and de-swelling of gel w.r.t. temperature resulting in the good stability on topical delivery. The thixotropy of any transdermal drug delivery system showed the clinical application in terms of penetration, muco-adhesion and spreadability of the gel system. The thixotropy outcomes of RCNGL showed decent dispersion and spreadability authenticating the potential transdermal clinical usage of RCNGL. The flow index assessment showed plastic behaviour of synthesized RCNGL over 90 days storage when equated with variable temperature range. The outcomes showed intense ascending and

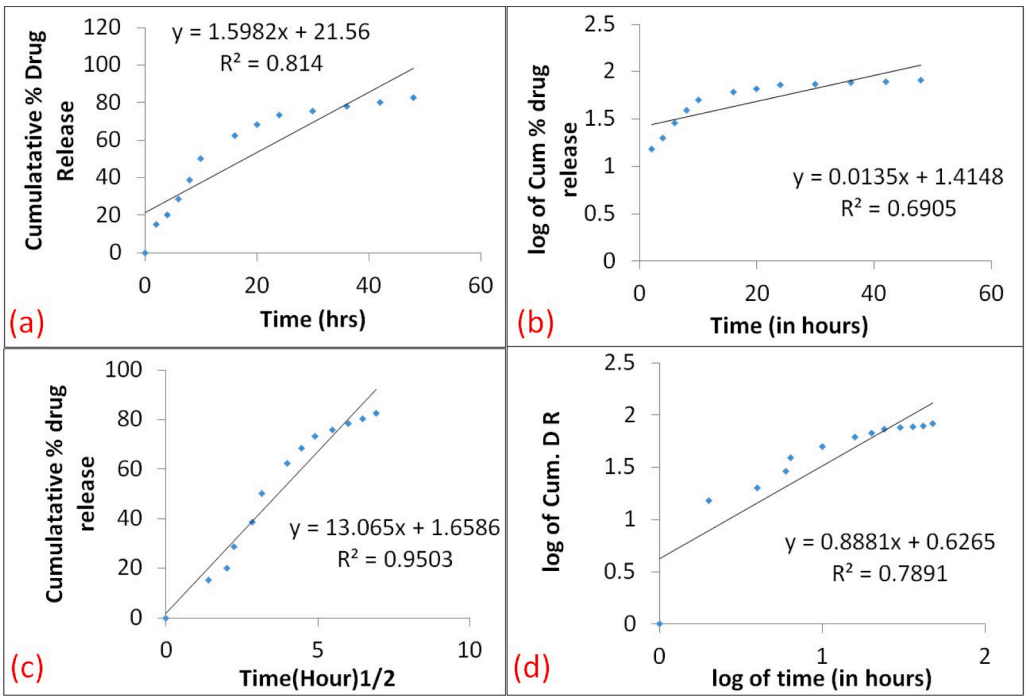


**Fig. 4.** Images a-d showing drug release kinetics by different model, (a) Zero order kinetics plot, (b) First order kinetics plot, (c) Higuchi model plot and (d) Korsemeyer - Peppas model release kinetic plot, (mean ± SD, n=3).

descending pattern of RCNGL due to the enhancement in kinetic energy of the molecules with increase in temperature. Therefore, the rheological pattern established the non-significant physiochemical and thermal instability of RCNGL over 90 days of storage and both 25 °C and 32 °C of temperature range revealing decent operational transdermal delivery when equated to 8 °C (cool temperature) and 45 °C (high temperature). Overall, the rheological outcomes validate the thermal and physiochemical stability of synthesized RCNGL over the 90 days of storage and varied temperature exposure conditions.

### *4.8. Drug Entrapment Assay*

The developed RCNGL was evaluated for the drug encapsulation efficiency. The RCNGL consist a varied polymer range, which influence greatly in the molecular weight and identity. This variation may affect the drug encapsulation of RCNGL. The RCNGL was evaluated on the basis of swelling and de-swelling phenomenon, higher the swelling ability and porosity, more will be the drug encapsulation. The RCNGL showed about 67.53 ±1.05 % drug loading efficiency when evaluated qualitatively by the UV spectroscopic method. The drug loading efficiency of RCNGL was found significant as an exterior chitosan aid in the better swelling (the tendency of absorption large amount of water) resulting in decent drug encapsulation potential of the synthesized RCNGL. The high entrapment of RCNGL linked to the outer carboxylate molecule of chitosan, higher porosity and the significant swelling tends to accommodate more amount of Risendronate.

### *4.9. Sol gel fraction and Porosity Analysis*

The percentage yield of synthesized RCNGL was found to be more than 70%, establishing decent particle entrapment efficiency and stabilized gel system. The deviation in the sol gel fraction and porosity is recorded and demonstrated in the fig. 3 a-c. The optimized chitosan and Sodium tripolyphosphate resulted in stabled RCNGL synthesis and significant percentage yield due to the increment in constructive density. Optimized chitosan concentration (0.4 % w/v) for synthesis of NPs resulted in stable particles system with decent particle size of below 200 nm. Elevation of chitosan concentration above 0.6% w/v resulted in the increased particle size and surface adsorption leading to the insignificant percentage yield and stability. Increased concentration of TPP above 0.5% w/v leads to the increased particle size and surface density due to availability of the larger surface area to cross linked with polymers. Therefore, the optimization of cross linker concentration is crucial to obtain the desired particle size for operational transdermal delivery. The concentration of Pluronic F-127 also impart crucial roles in stable gel formation with significant RCNGL yield. At low concentration between 5-10 % w/v, the gel yield declines drastically due to the less surface density, whereas at intermediate concentration between 10-15% w/v, the stability of gel was insignificant due to the formation of multi molecular micelles leading to the inadequate physiochemical stability. At optimized concentrations of Pluronic F-127 above 20% w/v the RCNGL showed a noteworthy yield of above 70% and enhanced physiochemical stability. The porosity of the synthesized RCNGL deviates significantly by chitosan and PF 127 concentration (Fig. S-B). Elevated chitosan concentration was resulting in the increased porosity of above 80% due to hydrophilic nature and have a tendency to absorb large amount of water. In contrast to polymers the co-polymer concentration of Pluronic F-127 showed increased porosity of above 85% in the gel structure due to the elevated hydrophilic nature resulting in stable 3D gel network for the effective topical application.

### *4.10. In vitro drug release studies*

The *in-vitro* drug release of free drug Risendronate and RCNGL were accomplished by using the dialysis bag method in PBS (phosphate buffered saline) solution at different pH 5.0 at 37 °C to mimic the skin microenvironment. The drug release profile of the free drug Risendronate and synthesized RCNGL at pH 5 was elaborated in the fig. 3 d. The RCNGL drug discharge pattern exhibited the biphasic behaviour with early bursting of nanoparticles in initial 1-10 h followed by the slow and sustained release. This initial discharge of drug from the RCNGL is due to the hydrophilic nature of chitosan on the exterior of the NPs showing a tendency to absorbing large amounts of water leading in the early degradation of nanoparticles particles via hydrolysis mechanism. At

**Table 2**
Interpretation of $R^2$ values and rate constants (K) of release kinetics of NPs, (mean ± SD, n=3).

| S. No. | Kinetic Models | Correlation value ($R^2$) | Release exponent (n) |
|---|---|---|---|
| 1 | Zero order model | 0.814 | —— |
| 2 | First order model | 0.690 | —— |
| 3 | Higuchi model | 0.950 | —— |
| 4 | Korsmeyer–Peppas model | 0.789 | 0.88 |

Note: In the above table "**$R^2$**" is correlation value and "**n**" is release exponent.

slightly acidic pH 5 the drug release was 80-85% due to the pH sensitivity of chitosan in a slightly acidic environment which tends to degrade the outer chitosan coating leading in the optimum release of drug. The free drug Risendronate at pH 5, showed more than 75 % in early 1-8 hours due to early adsorption of un-boundness and exposure to dissolution media. After 10 h the risendronate release was negligible due to fully exhaust in early stage of dissolution. At slightly acidic pH 5, the drug release is optimum and noteworthy in 48 h ascertaining the pH responsive nature of RCNGL leading to the controlled release of risendronate on transdermal delivery. In-vitro drug release studies were carried out using dialysis bag method for different mathematical kinetic models. For kinetic study of formulated drug NPs, the plots were made for Zero order kinetic model (cumulative % drug release vs time), First order kinetic model (log of cumulative % drug remaining vs time), Higuchi model cumulative (% drug release vs square root of time) and Korsmeyer– Peppas model (log cumulative % drug release vs log time). Plots of above mentioned models are shown in Fig. 4 a-d and results are summarized in Table 2.

### 4.11. Stability studies

The synthesized RCNGL nanoformulation was evaluated for the stability at 04 °C, 25 °C and 40 °C of varied temperatures and stored for 15, 30 and 45 days for change in the particle size and residual drug content (Fig. 3 e-f). The particle size and surface morphology of the RCNGL were evaluated by the zeta sizer measurement and optical microscopy using a calibrated ocular micrometer respectively. As the temperature increases from 4 °C to 40 °C the particle size increases drastically with the significant loss of encapsulated drug over varied storage duration (from 15 to 45 days). During the initial storage the deviation in particle size and the residual drug content was minimal, as the storage time increases, the variation in particle size and residual drug content was noteworthy in moderate (25 °C) and high temperature (40 °C) range (Fig. S F & G). The outcomes showed a significant elevation at higher temperature (40 °C > 300 nm) with severely swelled morphology on 45 days of storage. At 25 °C, the particle size was nominal increased (25 °C > 250 nm) with slight swelling whereas at low temperature 4 °C there is no change in the particle size and no sign of swelling was found. The residual drug content was measured spectrophotometrically suggesting a significant decline in the total risendronate encapsulation (50%) at higher temperature showing the heavy leakage and pores formation due to the elevated temperature. At moderate temperature (25 °C) the total residual drug content was non-significant (65%) due to the slight swelling and slow leakage. Whereas, at low temperature (4 °C) a negligible loss of encapsulated drug was found after the 45 days of storage, exhibiting the significant stability of RCNGL system. Overall, the stability studies of the developed RCNGL at varying temperature range and storage duration suggested the decent physiochemical stability at low and room temperature.

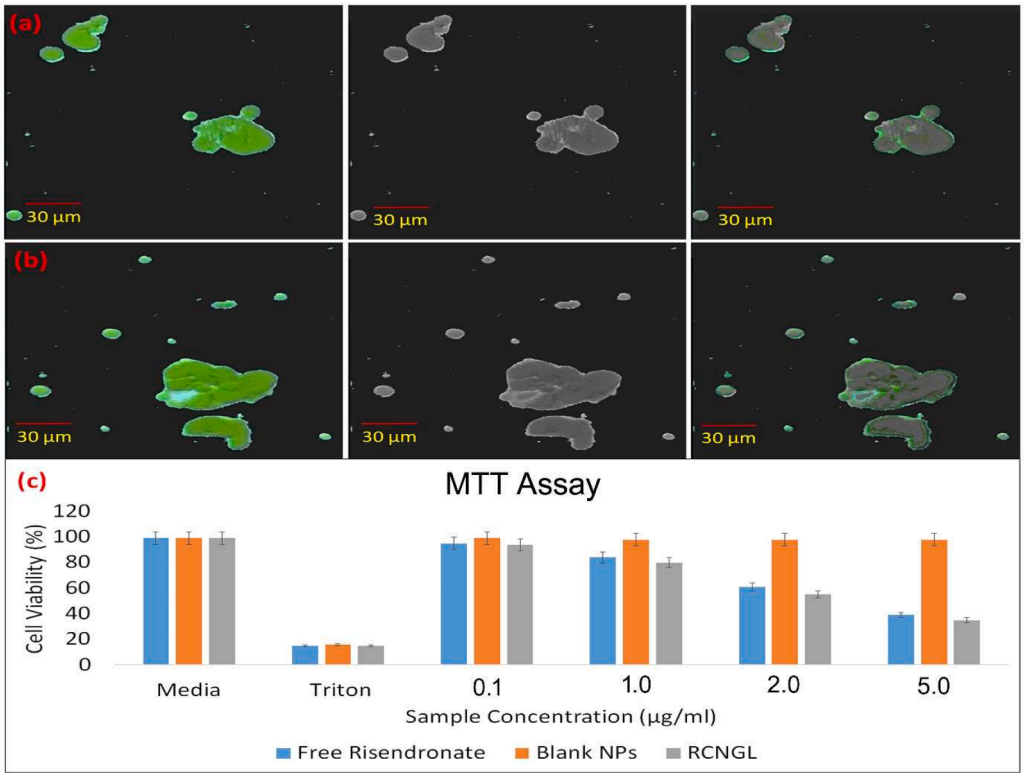


**Fig. 5.** Images a-b exhibiting CLSM localization and uptake analysis on Normal Human dermal fibroblast (NHDF) cell line post treatment with phase contrast microscopy and merge cell images treated with (a) Free Risendronate, (b) RCNGL at 30µm scale bar after 12 h incubation respectively, whereas image c showing MTT cell viability analysis on NHDF cell of different samples at 24 h incubation *p<0.05 and *p<0.01 compared to the untreated cell, (mean + SD, n=3).

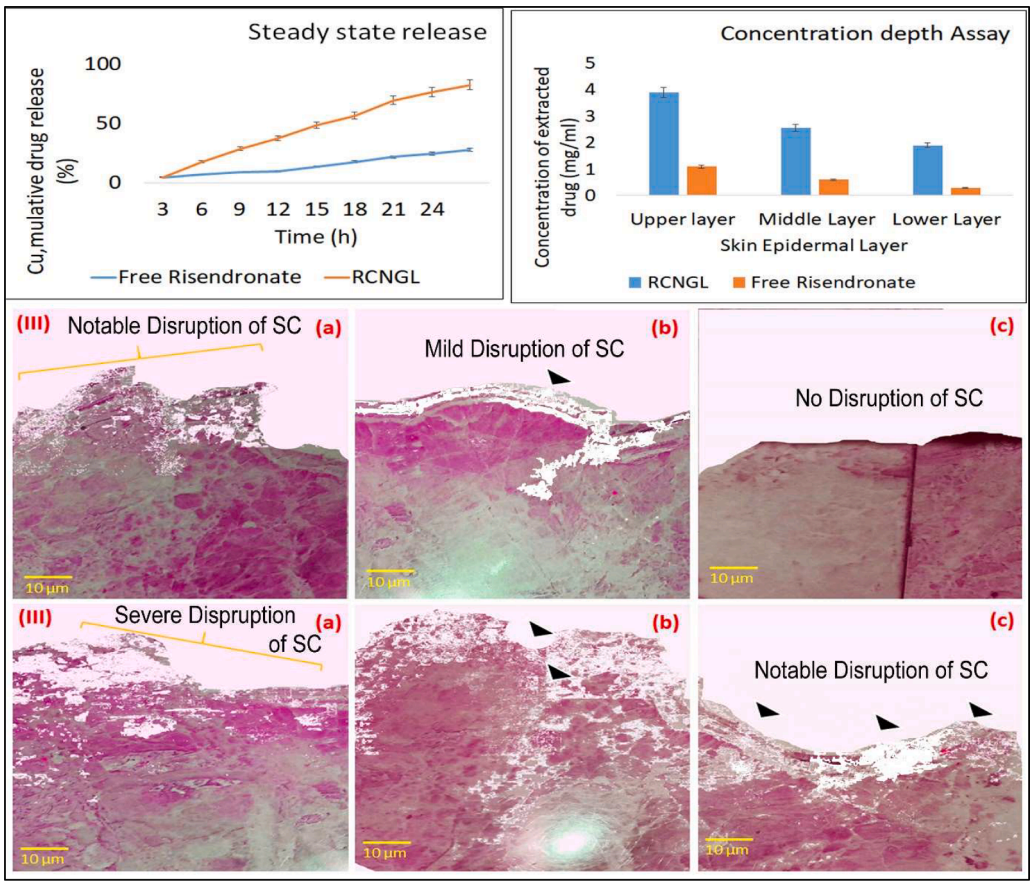


**Fig. 6.** Image (I-II) showing steady state flux and showing concentration depth assessment of extracted Risendronate at various epidermal layers of mouse tissue treated with free Risendronate and RCNGL at 10µm scale bar, post 24 h of ex vivo experimentation employing Franz diffusion cell assembly, images III-IV (a, b &c) displaying histopathology and permeating potential of free Risendronate (III, a-c) and RCNGL (IV, a-c) treated mouse tissue at different epidermal layer visualized at 100X lens magnification using light microscope (Olympus, Japan) (n=3, data expressed as average ± SD,*denotes p<0.01).

### *4.12. Cytotoxicity Studies*

#### *4.12.1. Cell Uptake & Distribution Assay by CLSM*

The Confocal Laser Scanning Microscopy (CLSM) displayed significant uptake and distribution of RCNGL evaluated on NHDF cell lines. The CLSM outcomes exhibited noteworthy internalization and distribution of NHDF. The fluorescent intensity demonstrated sharp ratification of RCNGL around the nucleus region of cells (marked red arrow). The cellular uptake images of RCNGL revealed large patches occurrence with expanded sign of fluorescence at the outer cell surface. The intense fluorescence signals displayed by RCNGL on NHDF cell line are the sign of vesicular localization of RCNGLdemonstrating endocytic pathway progression. The native vesicular uptake also exhibiting pinocytosis mechanism and non-phagocytosis phenomenon of RCNGL on NHDF cell line (Fig. 5 a-b). Therefore, the CLSM outcomes significantly demonstrated size dependent internalization uptake and distribution of RCNGL.

#### *4.12.2. Cytotoxicity Assessment by MTT Assay*

The MTT assay demonstrated that free drug Risendronate, blank NPs and RCNGL are cytocompatible at all concentration employed in cytotoxicity measurement against the NHDF cell line. The MTT results noteworthy showed that RCNGL exhibited sharp toxicity towards the NHDF cell when compared with normal control. The cytotoxicity of RCNGL towards NHDF cell was established statistically noteworthy compared to normal control ($p<0.01$) (Fig. 4 e). The plain risendronate showed optimum toxicity towards NHDF cell due to direct viability of free drug. The MTT assay noteworthy exhibited conservation of cell integrity devoid of any alteration cell microenvironment processes. The significant cytotoxicity of RCNGL leads to better development of the alternate nanocarrier over the existing one for the enhanced topical drug delivery system.

### *4.13. Ex-Vivo skin permeation evaluation*

#### *4.13.1. Skin penetration by steady state flux*

The *ex-vivo* permeation results elaborated enhanced diffusion of RCNGL by Franz diffusion cell employed against skin tissue compared to free risendronate solution under a UV lamp (Fig. 6-I). The UV spectrophotometry analysis illustrated noteworthy diffusion of RCNGL depicting 70% drug release compared to free drug solution in the 24 h experiment. The flux rate of RCNGL compared to free drug solution is 3 folds better and found significant ($P< 0.01$). There exists a symbiotic relationship between diffusion constant (D) and steady state flux (J). The elevation in D is directly proportional to the J due to enhanced disruption of corneocytes leading to the better steady state flux (J). The transcellular and intracellular transport via hair follicle pathway and sweat glands pathway respectively, plays a vital role in efficient penetration and diffusion of RCNGL. Therefore, the RCNGL system showed significant and enhanced penetration potential compared to free drug solution when analyzed by *ex-vivo* penetration assay.

#### *4.13.2. Concentration-Depth Profile*

The RCNGL concentration depth profile showed very sharp uptake and retention of capecitabine from gel matrix in the skin epidermal layer. The experimental exposure of mouse tissue confirmed significant

diffusion of risendronate from RCNGL when compared with free drug solution. The concentration depth analysis validated steady state flux depicting enhanced penetration and retention efficacy of RCNGL at different epidermal layer. The fluorescent microscopic images showed noteworthy diffusion and retention at upper epidermal layer compared to middle and lower layer (Fig. 6-II). The penetration and retention potential of RCNGL at all epidermal layers was twice better than free drug solution and found significant ($P<0.01$). The ionic interaction between positively charged RCNGL with negatively charged cell membrane caused efficient binding to skin cell.

#### *4.13.3. Histology Profile*

The *ex-vivo* histology profile showed noteworthy permeation potential of RCNGL compared to free drug solution. The histology evaluation of RCNGL displayed significant disruption of the squamous layer with the slackening of lipid bilayers compared to free drug solution treated tissue. The lipid bilayer disruption of RCNGL treated tissue is higher due to the hydrophilic nature of risendronate (Fig. 6 III-IV). The disruption of SC validated the better penetration strength of RCNGL without generating any annoying eruptions or erythema and swelling of SC. The e*x-vivo* histological assay confirmed stable flux and augmented penetration potential of RCNGL. The histology results significantly confirmed the enhanced diffusion, skin penetration and retention potential of RCNGL. Overall, the *ex-vivo* outcome opens the novel alternative transdermal nanotherapy against numerous disorders with low dose interval and negligible cellular toxicity.

## 5. Conclusion

The transdermal drug delivery system in the management of osteoporosis open new avenue with the basis of nanotechnology as Osteoporosis provokes concern about their long-term safety. An innovative system has been discovered and contrived utilizing existing synthesis techniques and established as an anti-osteoporosis agent. The RCNGL was showed enhanced penetration potential mediated by mouse skin tissue ex-vivo experimentation, exhibiting sustained release of risendronate at defined entrapment efficiency on passive targeting. The concluding RCNGL was synthesized by optimizing the process and formulation parameters for obtaining stable and nanosized particles exhibiting stable release kinetics models. Optimized RCNGL possess better penetration and transportation across SC and diffuses via skin lipids for enhanced retention and distribution at the targeted site. The current *in-vitro* and *ex-vivo* outcomes employing mouse tissue discovered the effectiveness and transdermal viability of RCNGL in the management of Osteoporosis. Overall RCNGL is discovered as an encouraging alternative transdermal contender with remarked clinical translational efficiency.

## Ethical Approval

Not applicable.

## Informed consent

This article does not contain any studies with human participants.

## Funding

Nil.

## CRediT authorship contribution statement

**Sandhya Pathak:** Conceptualization, Data curation, Writing – original draft. **Prashant Sahu:** Formal analysis, Investigation. **J.P. Shabaaz Begum:** Formal analysis, Investigation. **Sushil K Kashaw:** Formal analysis, Investigation. **Archana Pandey:** Supervision. **Prabhakar Semwal:** Writing – review & editing. **Rohit Sharma:** Writing – review & editing.

## Declaration of competing interest

The authors declare that they have no known competing financial interests or personal relationships that could have appeared to influence the work reported in this paper.

## Data availability

Data will be made available on request.

## Acknowledgements

The authors are grateful to AIIMS, New Delhi and IISER (Bhopal) for qualitative analysis and DLS studies. We acknowledge Sophisticated Instrumentation Centre (SIC), Dr.HarisinghGour Vishwavidyalaya (A Central University), Sagar for Optical analysis and structural studies work. Thanks conveyed to SRL laboratory, Gurgaon, India for skin tissue work studies along with providing us the histology study facilities. We pay our sincere thanks to University Grant commission for providing PhD fellowship in the smooth completion of research work.

## Refrences

Araujo, P. (2009). Key aspects of analytical method validation and linearity evaluation. *Journal of chromatography B, 877*(23), 2224–2234.

Ballarin, B., Galli, S., Mogavero, F., & Morigi, M. (2011). Effect of cationic charge and hydrophobic index of cellulose-based polymers on the semipermanent dyestuff process for hair. *International journal of cosmetic science, 33*(3), 228–233.

Borah, P. K., Deka, S. C., & Duary, R. K. (2017). Effect of repeated cycled crystallization on digestibility and molecular structure of glutinous Bora rice starch. *Food chemistry, 223*, 31–39.

Choi, A., Gang, H., Chun, I., & Gwak, H. (2008). The effects of fatty acids in propylene glycol on the percutaneous absorption of alendronate across the excised hairless mouse skin. *International Journal of Pharmaceutics, 357*(1-2), 126–131.

Cione, A. P. P., Liberale, M. J., & Silva, P. M.d. (2010). Development and validation of an HPLC method for stability evaluation of nystatin. *Brazilian Journal of Pharmaceutical Sciences, 46*, 305–310.

Costa, P., & Lobo, J. M. S. (2001). Modeling and comparison of dissolution profiles. *European journal of pharmaceutical sciences, 13*(2), 123–133.

Damle, M., & Birajdar, L. B. (2015). *DEVELOPMENT AND VALIDATION OF STABILITY-INDICATING HPLC METHOD FOR ESTIMATION OF RISEDRONATE SODIUM*.

Das, D., Sahu, P., Chaurasia, A., Mishra, V. K., & Kashaw, S. K. (2018). Nanoemulsion: The Emerging Contrivance in the Field of Nanotechnology. *Nanoscience & Nanotechnology-Asia, 8*(2), 146–171.

Dey, S., Banerjee, U., Sen, T., & Shankar, V. (2011). Formulation and in vitro evaluation of transdermal matrix patches of diclofenac sodium. *Journal of Pharmacy Research, 4*. JPR_11_712.

Dissette, V., Bozzi, P., Bignozzi, C. A., Dalpiaz, A., Ferraro, L., Beggiato, S., & Pasti, L. (2010). Particulate adducts based on sodium risedronate and titanium dioxide for the bioavailability enhancement of oral administered bisphosphonates. *European journal of pharmaceutical sciences, 41*(2), 328–336.

Fazil, M., Baboota, S., Sahni, J. K., Ameeduzzafar, & Ali, J (2015). Bisphosphonates: therapeutics potential and recent advances in drug delivery. *Drug Delivery, 22*(1), 1–9.

Fleisch, H. (2000). *Bisphosphonates in bone disease: from the laboratory to the patient.* Elsevier.

Garzoni, L. R., Waghabi, M. C., Baptista, M. M., De Castro, S. L., Maria de Nazareth, L. M., Britto, C. C., & Urbina, J. A. (2004). Antiparasitic activity of risedronate in a murine model of acute Chagas' disease. *International journal of antimicrobial agents, 23*(3), 286–290.

Guyot, M., & Fawaz, F. (2000). Design and in vitro evaluation of adhesive matrix for transdermal delivery of propranolol. *International Journal of Pharmaceutics, 204*(1-2), 171–182.

Higuchi, T. (1963). MECHANISM OF SUSTAINED-ACTION MEDICATION. THEORETICAL ANALYSIS OF RATE OF RELEASE OF SOLID DRUGS DISPERSED IN SOLID MATRICES. *J Pharm Sci, 52*, 1145–1149.

Hirabayashi, H., Sawamoto, T., Fujisaki, J., Tokunaga, Y., Kimura, S., & Hata, T. (2002). Dose-dependent pharmacokinetics and disposition of bisphosphonic prodrug of diclofenac based on osteotropic drug delivery system (ODDS). *Biopharmaceutics & drug disposition, 23*(8), 307–315.

Kusamori, K., Katsumi, H., Abe, M., Ueda, A., Sakai, R., Hayashi, R., & Sakane, T. (2010). Development of a novel transdermal patch of alendronate, a nitrogen-containing bisphosphonate, for the treatment of osteoporosis. *Journal of Bone and Mineral Research, 25*(12), 2582–2591.

Li, Y., Pang, H., Guo, Z., Lin, L., Dong, Y., Li, G., & Wu, C. (2014). Interactions between drugs and polymers influencing hot melt extrusion. *J Pharm Pharmacol, 66*(2), 148–166.

Liu, C.-H., Chang, F.-Y., & Hung, D.-K. (2011). Terpene microemulsions for transdermal curcumin delivery: effects of terpenes and cosurfactants. *Colloids and Surfaces B: Biointerfaces, 82*(1), 63–70.

Nam, S. H., Xu, Y. J., Nam, H., Jin, G.-w., Jeong, Y., An, S., & Park, J.-S. (2011). Ion pairs of risedronate for transdermal delivery and enhanced permeation rate on hairless mouse skin. *International Journal of Pharmaceutics, 419*(1-2), 114–120.

Ngo, D.-N., Lee, S.-H., Kim, M.-M., & Kim, S.-K. (2009). Production of chitin oligosaccharides with different molecular weights and their antioxidant effect in RAW 264.7 cells. *Journal of Functional Foods, 1*(2), 188–198.

Olkin, I., & Pratt, J. W. (1958). Unbiased estimation of certain correlation coefficients. *The annals of mathematical statistics*, 201–211.

Papapetrou, P. D. (2009). Bisphosphonate-associated adverse events. *Hormones, 8*(2), 96–110.

Pasqualone, M., Oberti, T. G., Andreetta, H. A., & Cortizo, M. S. (2013). Fumarate copolymers-based membranes overlooking future transdermal delivery devices: synthesis and properties. *Journal of Materials Science: Materials in Medicine, 24*, 1683–1692.

Peppas, N. (1985). Analysis of Fickian and non-Fickian drug release from polymers. *Pharmaceutica Acta Helvetiae, 60*(4), 110–111.

Prashant Sahu, S. S., Iyer, Arun K., & Kashaw, Sushil K. (2017). Nanogels: The Emerging Carrier in Drug Delivery System. In S. T. Jince Thomas, & Jiya Jose (Eds.), *Recent Trends in Nanomedicine and Tissue Engineering* (p. 36). The Netherlands: River Publishers.

Qiu, Y., Chen, Y., Zhang, G. G., Yu, L., & Mantri, R. V. (2016). *Developing solid oral dosage forms: pharmaceutical theory and practice*. Academic press.

Rao, D., Dandala, R., Lenin, R., Sivakumaran, M., Shivashankar, S., & Naidub, A. (2007). A facile one pot synthesis of bisphosphonic acids and their sodium salts from nitriles. *Arkivoc, 14*, 34–38.

Ritger, P. L., & Peppas, N. A. (1987). A simple equation for description of solute release I. Fickian and non-fickian release from non-swellable devices in the form of slabs, spheres, cylinders or discs. *Journal of controlled release, 5*(1), 23–36.

Sahu, P., Das, D., Mishra, V. K., Kashaw, V., & Kashaw, S. K. (2017). Nanoemulsion: a novel eon in cancer chemotherapy. *Mini reviews in medicinal chemistry, 17*(18), 1778–1792.

Sahu, P., Kashaw, S. K., Jain, S., Sau, S., & Iyer, A. K. (2017). Assessment of penetration potential of pH responsive double walled biodegradable nanogels coated with eucalyptus oil for the controlled delivery of 5-fluorouracil: In vitro and ex vivo studies. *Journal of controlled release, 253*, 122–136.

Sahu, P., Kashaw, S. K., Kushwah, V., Sau, S., Jain, S., & Iyer, A. K. (2017). pH responsive biodegradable nanogels for sustained release of bleomycin. *Bioorganic & medicinal chemistry, 25*(17), 4595–4613.

Sahu, P., Kashaw, S. K., Sau, S., Kushwah, V., Jain, S., Agrawal, R. K., & Iyer, A. K. (2019). pH responsive 5-fluorouracil loaded biocompatible nanogels for topical chemotherapy of aggressive melanoma. *Colloids and Surfaces B: Biointerfaces, 174*, 232–245.

Sahu, P., Sushil, K., Samaresh, S., & Arun, K. (2017). Stimuli-responsive bio-hybrid nanogels: an emerging platform in medicinal arena. *J Controlled Rele, 107*(1), 143–157.

Schenk, R., Eggli, P., Fleisch, H., & Rosini, S. (1986). Quantitative morphometric evaluation of the inhibitory activity of new aminobisphosphonates on bone resorption in the rat. *Calcified tissue international, 38*, 342–349.

Sigua-Rodriguez, E. A., da Costa Ribeiro, R., de Brito, A. C., Alvarez-Pinzon, N., & de Albergaria-Barbosa, J. R. (2014). Bisphosphonate-related osteonecrosis of the jaw: a review of the literature. *Int J Dent, 2014*, Article 192320.

Stamatialis, D. F., Papenburg, B. J., Gironés, M., Saiful, S., Bettahalli, S. N., Schmitmeier, S., & Wessling, M. (2008). Medical applications of membranes: Drug delivery, artificial organs and tissue engineering. *Journal of Membrane Science, 308* (1-2), 1–34.

Tanwar, Y., Chauhan, C., & Sharma, A. (2007). Development and evaluation of carvedilol transdermal patches. *Acta pharmaceutica, 57*(2), 151.

Tella, S. H., & Gallagher, J. C. (2014). Prevention and treatment of postmenopausal osteoporosis. *The Journal of steroid biochemistry and molecular biology, 142*, 155–170.

Ulbrich, K., Hola, K., Subr, V., Bakandritsos, A., Tucek, J., & Zboril, R. (2016). Targeted drug delivery with polymers and magnetic nanoparticles: covalent and noncovalent approaches, release control, and clinical studies. *Chemical reviews, 116*(9), 5338–5431.

Watts, M. R., Ellims, A. H., & Eccleston, D. S. (2014). Acute myopericarditis following intravenous zoledronic acid for the treatment of Paget's disease. *The Medical Journal of Australia, 200*(3), 150.

Wong, S., Zhao, J., Cao, C., Wong, C. K., Kuchel, R. P., De Luca, S., & Ho, J. (2019). Just add sugar for carbohydrate induced self-assembly of curcumin. *Nature Communications, 10*(1), 582.

Zhang, Y., Wei, L., Miron, R. J., Shi, B., & Bian, Z. (2016). Bone scaffolds loaded with siRNA-Semaphorin4d for the treatment of osteoporosis related bone defects. *Scientific Reports, 6*(1), 26925.